

Development and Preliminary Data of Novel Integrated Optical Micro-Force Sensing Tools for Retinal Microsurgery

Zhenglong Sun, Marcin Balicki, *Student Member, IEEE*, Jin Kang, *Member, IEEE* James Handa, MD, Russell Taylor, *Fellow, IEEE*, and Iulian Iordachita, *Member, IEEE*

Abstract—This paper reports the development of novel micro-force sensing tools for retinal microsurgery. Retinal microsurgery requires extremely delicate manipulation of retinal tissue, and tool-to-tissue interaction forces are frequently below human perceptual thresholds. Further, the interaction between the tool shaft and sclera makes accurate sensing of forces exerted on the retina very difficult with previously developed force sensing schemes, in which the sensor is located outside the eye. In the work reported here, we incorporate 160 μm Fiber Bragg Grating (FBG) strain sensors into the tool shaft to sense forces distal to the sclera. The sensor is applicable both with robotically manipulated and freehand tools. Preliminary results with a 1 degree-of-freedom (DOF) sensor have demonstrated 0.25 mN resolution, and work is underway to develop 2 and 3 DOF tools. The design and analysis of the force sensing tool is presented with preliminary testing data and some initial experiments using the tool with both freehand and robotic manipulation.

I. INTRODUCTION

MANY clinical procedures involve manipulation of extremely small, delicate tissue structures. Retinal microsurgery is a particular example of such procedures. The manipulation of vitreoretinal structures inside the eye poses enormous challenges, due to tissue delicacy, surgical inaccessibility, suboptimal instrumentation for visualization, and potential for irreversible damage.

In current practice, retinal surgery is performed under a surgical microscope. Small (20-25 gauge) surgical instruments are inserted through the sclera of the eye through a small number (typically, 2-3) of sclerotomy sites. The main technical limitations in vitreoretinal surgery are: 1) inadequate spatial resolution and depth perception of microstructures to identify tissue planes, 2) imprecise movements during micromanipulation of tissue due to physiological tremor and 3) lack of force sensing since the movements required for dissection are below the surgeon's sensory threshold. These factors make vitreoretinal surgery

Manuscript received September 15, 2008. This work was supported in part by the U.S. National Science Foundation under Cooperative Agreement EEC9731478, in part by the National Institutes of Health under BRP 1 R01 EB 007969-01 A1, and in part by Johns Hopkins internal funds.

The authors are affiliated with the Center for Computer-Integrated Surgical Systems and Technology (CISST ERC) at The Johns Hopkins University, 3400 N. Charles Street, Baltimore, Maryland 21218 USA. Corresponding Author: Iulian Iordachita iordachita@jhu.edu.

the most technically demanding ophthalmologic surgery, although these same technical factors are important to other microsurgical disciplines. These factors interact. Physiological tremor, which contributes to long operative times and which is exacerbated by fatigue, is a severe limiting factor in microsurgery [1]. Gupta et al. reported that a majority of retinal surgery is performed without force sensation of the interactions between retinal tissue and the surgical tool [2]. At JHU, we have had a long-standing research program intended to address these limitations through the use both of robots such as our steady-hand "Eye Robot" [3, 4] and through various "sensory substitution" schemes to provide the surgeon with feedback on tool-to-tissue forces that would otherwise be imperceptible.

There have been several investigations of force sensing for microsurgery or more general micromanipulation over the years. For example, Zhou *et al.* [5] developed a force sensing scheme relying on measuring the deflection of an optical beam. Kim *et al.* [6] developed multi-axis MEMS force sensors in an approximately 3 x 5 x 0.5 mm form factor. Menciassi *et al.* [7] developed a 15.5 mm micro-gripper with integrated strain gauge sensors.

Early work at the CISST ERC by Gupta *et al.* [2] included use of a 1 DOF pick-like probe to measure forces in retinal surgery and to explore the feasibility of a simple auditory "sensory substitution" scheme to assist the surgeon in controlling these forces. They determined that 75% of these forces were less than 7.5 mN in magnitude and that only 19% of force events of this magnitude are felt by the surgeon. Subsequently, Berkelman et al. developed a 3 DOF force sensor [8, 9] for use in ENT and eye applications with the JHU "Steady Hand" microsurgery system. Jagtap & Riviere [10] incorporated this sensor into a hand-held instrument and used it to measure forces in retinal tasks both on cadaveric pig retinas and in-vivo rabbit eyes. Experience with this instrument shows that in-vivo measurements are indeed feasible, but that discrimination between forces applied at the tool tip and forces from contact with the sclera may be a challenge if the force sensing is done proximal to the sclerotomy point.

These prior approaches pose a number of limitations retinal microsurgery applications. With the exception of [2], which used a strain gauge along the tool shaft, the sensor "packages" are too large to be incorporated easily into the portion of the microsurgical tool that is inside the eye. Placing a multi-axis force sensor in the tool handle, as was done in [8, 9] necessarily introduces significant sclera-to-instrument force

disturbances that can completely swamp the tool-to-tissue force measurements. Fabricating custom micro-MEMS sensors into the actual tool tip (e.g., into a 0.5 mm cutter blade or tweezers tip) is conceptually possible, but poses numerous fabrication, assembly, and interfacing problems.

These considerations led us to explore approaches in which sensors could be mounted along the portion of the tool shaft inside the eye. We looked at several sensing technologies, including conventional strain gauges, but settled on Fiber Bragg Grating (FBG) strain sensors. Optical fiber sensors are small (75-200 μ m diameter), extremely precise, stable, relatively inexpensive, easy to build into to \sim 1mm diameter tools, easy to interface to computers, relatively easy to sterilize, and immune to electrical noise. In addition, expertise gained in integrating FBGs into our tools could be readily transferred to other fiber-optic sensors and devices for microsurgery, as well as into other robotic and sensing applications in our laboratory.

In subsequent sections, we will describe our design requirements. We will then describe an initial 1 DOF prototype tool implementation present its calibration procedure & performance results, and will briefly describe our concept for a 2 DOF tool, which is currently being constructed. Finally, we will present some preliminary results using our 1 DOF prototypes with both hand-held and robotically manipulated tools.

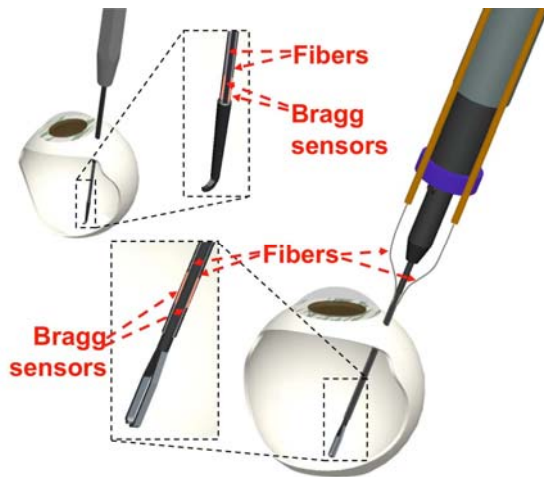


Fig. 1. Optical fiber force sensing concepts

II. OPTICAL MICRO-FORCE SENSING TOOL

The design of the force sensing surgical instrument has to meet both form factor constraints and measurement resolution requirements. The geometry of the surgical environment inside of the eye dictates the sensing element location, which should be close to the distal end of the tool. The sensor should not compromise the overall size of the instrument, and the device should have the capability of measuring forces at the tip with sub-mN resolution. The detail specifications of the goal are listed in Table I.

TABLE I Design specifications for the force sensing tool

Tool shaft diameter	< 1 millimeter
Tool shaft length	> 30 millimeter
Force Resolution at tip	\sim 0.25 millinewton
Sampling Rate	> 100 Hz

A. Fiber Optic Strain Sensing

In order to meet these design criteria, a fiber optic based strain measurement technology was chosen. Optical fibers are well adapted for integration into rigid tubular ophthalmology instruments. Typical fiber diameter is less than 1/6 of the standard instrument's diameter. Furthermore, it is immune to electrical noise and also can be biocompatible.

A single optical Fiber Bragg Grating (FBG) strain sensor is employed in the solution presented here. FBG causes a periodic perturbation of the refractive index along the fiber length. The grating is formed inside of the photosensitive fiber by exposure to an intense optical interference pattern, which effectively creates a wavelength specific dielectric mirror inside of the fiber core. This characteristic Bragg wavelength shifts due to modal index or grating pitch change from physical deformation caused by strain or temperature change. The shift can be precisely measured in real time. This technology has been used in a number of important application areas ranging from structural monitoring to chemical sensing [11].

B. Design and Fabrication

To mimic the 25 gauge ophthalmic instruments a 50 mm long titanium wire with 0.5mm diameter was prepared as the tool body. To determine the sensors geometric dimensions and material properties required to attain the necessary sensitivity, the sensor was modeled using a simple cantilever beam bending. Titanium was selected to provide the tool necessary toughness and relative large flexibility. To integrate the optical fiber into the shaft, a square section channel (160 \times 160 μ m) was machined into the surface along shaft's axial direction (Figure 2).

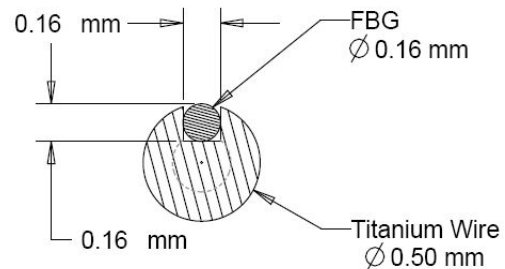


Fig. 2. Integrated 1-axis force sensing tool.

A customized FBG sensor, OS110, from Micron Optics, Inc. (Atlanta, GA) was used for this device. The fiber is 160 μ m in diameter. The FBG sensing region has 1550nm central wavelength. The location of the fiber's strain sensing region is 10mm long and is located 5mm from the end of the fiber.

This optimizes the force sensing sensitivity at the distal end of the tool while avoiding interference from contact with the sclera. This considers the eyeball diameter, ~25mm, and the fact that tissue manipulation is on the opposite side of the eye from the entry ports.

The distal fiber section, ~30mm, was bonded in the titanium wire channel using solid epoxy M-Bond AE-10 adhesive system from Vishay Micro-Measurements. The rest of the fiber was shrink wrapped with heat shrink tubing to the proximal end of the titanium shaft. This assembly was inserted through the pin vice, and tightened on the proximal end. Fig. 3 shows the integrated 1-axis force sensing tool prototype. The force resolution and update rate were checked by calibration.



Fig. 3. Integrated 1-axis force sensing tool.

A sm130 laser wavelength interrogator from Micron Optics Inc. was used to excite the sensor and analyze the returned spectrum. The device has a dynamic scan frequency up to 2 KHz and wavelength repeatability of 1 picometer. The data was collected using Matlab over an Ethernet connection at 200Hz.

C. Calibration

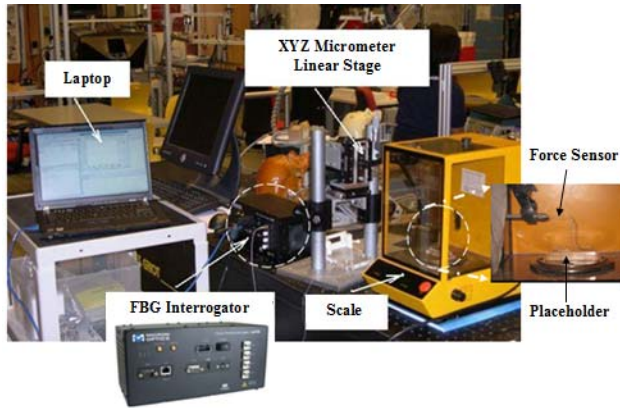


Fig. 4. Calibration Setup

Calibration was carried out in an electrically shielded analytical balance, Sartorius 1601 from Data Weighing Systems, Inc. (Elk Grove IL), which has a readability of 0.1 mg. An acrylic placeholder was placed on the balance below the tool tip. The tool was held horizontally by a pin vice, which attached to a 3-DOF linear translation stage. The tool was properly oriented so that the channel with the FBG sensor was either facing upwards or downwards in vertical plane. The tool shaft axis was positioned to be perpendicular to the placeholder's apex. The setup is shown in Fig. 4.

Through fine adjustment of the height of the vertical translation stage, the force exerted on the shaft tip can be calculated from the weight read from the analytical balance.

The resolution of the balance is 0.1mg, which is equivalent to 0.001mN in force for this setup. For every increment of 25mg in weight, the corresponding wavelength of the FBG sensor was recorded. Calibration was performed with the FBG facing downward and with the FBG facing upward, following by FBG oriented at horizontal position, corresponding to the neutral surface plane of the bending beam. The results are shown in Fig. 5. By changing the orientation, the surface with the embedded FBG will experience either tension (FBG downward) or compression (FBG upward). It is notable that the results show a linear relationship between the force exerted and the wavelength in both cases, and that the two calibration curves are almost symmetrical. And at horizontal position, the wavelength change under orthogonal force is negligible.

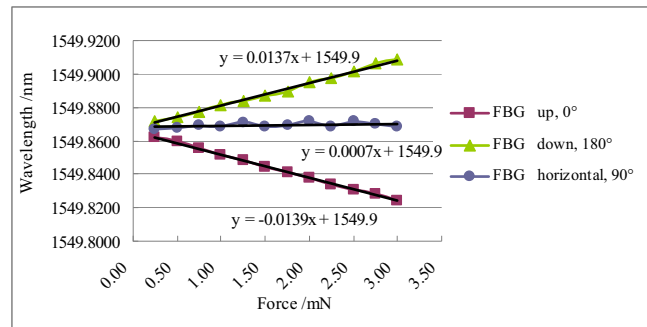


Fig. 5. Calibration results

From the calibration results we can conclude that the force resolution is adequate to meet the design goal of 0.25mN. At the point 1mm from the tool tip, the wavelength to force ratio is about 14 *picom*/mN. Calibrations were also performed at different loading points along the shaft. The results show that the wavelength to force ratio varies linearly along the tool shaft, which can be seen in Fig. 6. This also verifies the location of the effective FBG strain sensing region which ends 15 mm from the tool tip as designed.

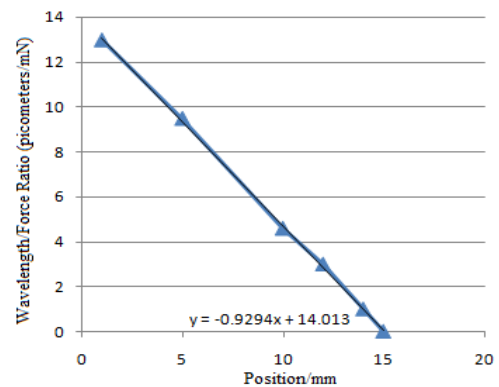


Fig. 6. Wavelength/Force ratio against position along the tool

D. Dynamic Characteristics

To characterize sensor's dynamic properties, a step input response was analyzed. The force sensor was preloaded with 20mN force using the setup in Fig 4. The load was then quickly removed while the signal was recorded at 2000Hz (Fig.7). The noise level is measured to be 0.04mN, yielding signal to noise ratio of 54 dB. The approximate signal rise and relaxation times are 3.5ms and 180ms, respectively and the impulse overshoot was measured to be 6.6 mN or 33 % of the steady-state value. Based on the impulse response of the device, the resonant frequency of the tool was measured to be 328Hz and damping constant of 47ms. From these measurements we can expect the overall sampling rate to be at least 5.5Hz. Maximum dynamic range of the device is estimated to be ~57 dB.

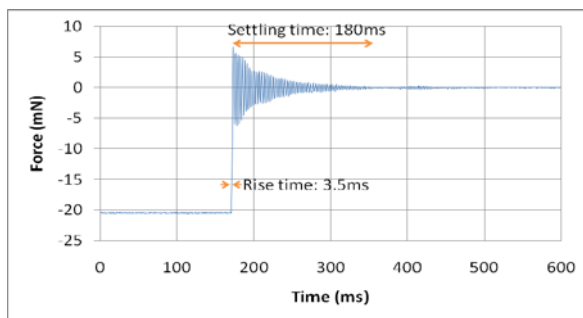


Fig. 7. Step Input Response after removing 20mN force.

III. FORCE MEASUREMENT IN DIFFERENT TASKS

Our main motivation for developing this sensor is to provide intraoperative feedback of tool-to-tissue manipulation forces in retinal microsurgery tasks such as epiretinal membrane peeling and retinal vein cannulation. For the reasons discussed above, such measurements have not been practical for millimeter-diameter tools inserted into the eye.

In this section, we report some initial pilot studies performed on realistic phantoms using our 1 DOF sensors. The purpose of these experiments is to demonstrate the ability of our sensor to provide useful information in a somewhat realistic environment, both with robotically manipulated and freehand instruments. These studies also provide valuable experience guiding the design of our multi-DOF sensing tools and for the development of sensory substitution and robotic force control methods for assisting the surgeon. Although results are presented for both robotic and freehand tool manipulation, these initial studies are not intended to demonstrate any relative advantages between robotic and freehand manipulation. Rather, they are intended to provide a basis for developing a variety of robotic and human interfaces that will eventually produce such advantages, compared to unassisted tool manipulation.

The calibration results proved the capability of tool to sense forces with 0.25mN resolution, however, to have a better idea about the amplitude of the interaction forces

during these tasks the following experiments were performed using the 1-axis force sensing prototype. During the experiments we have constructed the experimental setup such that the force application is inline with the sensing direction of the sensor. For a clinical application a 2DOF (in transverse plane) sensing is required. This is addressed in future work and builds on the initial proof of concept design presented here.

As suggested in [12], we use the chorioallantoic membrane (CAM) of a 12 day old chicken embryo as an eye phantom for the experiments. For comparison we have chosen to experiments were performed using both free hand and the Eye Robot. Wavelength shifts in the FBG sensor were recorded for each trial using a sampling frequency of 200 Hz.

In order to simulate a bent tip pipette an adapter was build that connects a straight tip micro-pipette to the 1-axis force sensing prototype. The adapter ensures that the force at the tool tip is in sensing plane of the sensor, as well as perpendicular to it. This matches the point of application of the force experienced during calibration. The assembly was done visually inspected under the microscope to have a best possible alignment.

The hook for membrane peeling experiment was similarly attached but with the long axis of the hook attached in parallel with the long axis of the force sensing prototype. Such arrangement optimizes the sensitivity to peeling forces when the force is applied perpendicular to the hook shaft.

Examples of the tool connections can be seen in Fig. 8.

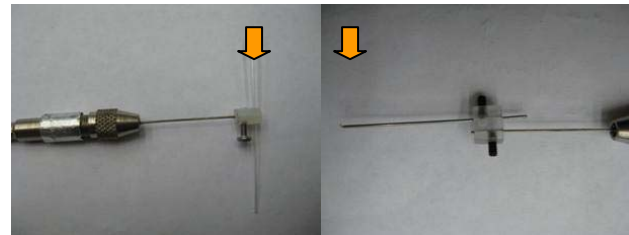


Fig. 8. Connector to different tools (left) straight micro-pipette, (right) hook. Arrows depict tissue force direction.

A. Vein Cannulation

Retinal vein cannulation can deliver medication to a microvessel, a method that has potential to treat clots in the retinal vasculature. However, currently it is not a standard of care in retinal microsurgery due to the low cannulation success rates. With the cooperative control Steady Hand Eye Robot, we have developed a protocol and successfully cannulated CAM veins (down to ~80 μ m) rapidly, reliably, and with minimal damage to the surrounding tissue. More details can be found in [4].

In this vein cannulation experiment, we followed a similar protocol. In this case, the injector syringe is not connected to the pipette and the user was requested to hold the tool for 10 seconds to simulate the time consumed for delivering the drug before moving the tool tip out of the vessel. The setup for the vein cannulation using the Eye Robot is shown in Fig. 8.



Fig. 9. (Left) Vein cannulation setup with freehand straight micro-pipette (Right) Membrane peeling setup on the Eye Robot with a customized hook, the inner shell membrane (ISM)

B. Membrane Peeling

Membrane peeling is clinical task to treat the Epiretinal Membrane (ERM). ERM is a cellophane-like membrane that forms over the macula. It is typically a slow-progressing problem that affects the central vision by causing blur and distortion. Typically this membrane is peeled to restore vision, a procedure considered to be of high risk. To simulate this, we performed the peeling on the inner shell membrane (ISM) in the chicken embryo. It is approximately $20\mu\text{m}$ thick, which lies on top of the CAM (Fig. 9). The protocol of peeling is that the subject keeps moving the hook along the membrane surface at an angle of $\sim 90^\circ$, slowly increasing the force until a tear is created, and then continuing to move along the surface to peel until the membrane slips off the hook.

C. Results and Discussion

Data was filtered internally by the FBG interrogator during the data collection. A sample moving average of 100 was applied. Example of force profiles in a single trial from vein cannulation and membrane peeling are shown in Fig. 10,11 respectively.

From the vein cannulation data, we can clearly observe a peak when the pipette is puncturing the vein wall to penetrate into the vessel. It can be seen that the signal with robot assistance is more stable and less noisy than the one by free hand. From the membrane peeling data, there is little difference in noise strength between free hand and with robot assistance. This implies that the hand tremor is more significant and has more influence in performance when it is in motion than keeping still.

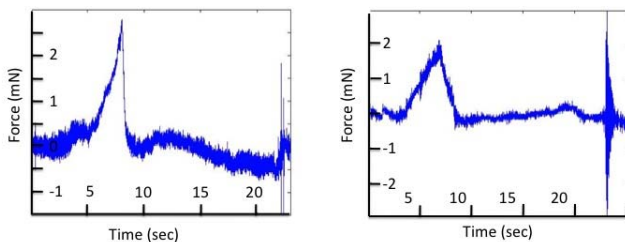


Fig. 10. Cannulation using straight pipette by free hand (Top), and Eye Robot assisted (Bottom)

However, when the pipette is taken out of the vessel, there

exist higher oscillating distortions in using the robot than by free hand, for both cannulation and peeling. By analyzing the signal in frequency domain, we found that the eye robot servo control induced micro-vibration in the force sensing tool. The plastic adapter connecting the force sensor and the pick or pipette will amplify the vibration especially when losing contact with tissue in tension. This vibration is found to be about 60Hz, 5 times higher than typical hand tremor frequency of 8-12Hz. The pulse response experienced during retraction may cause slight oscillations in the robot's control system dynamics. With a redesigned tool rather than using adapters, the mass at the tip should be significantly reduced, minimizing these oscillations.

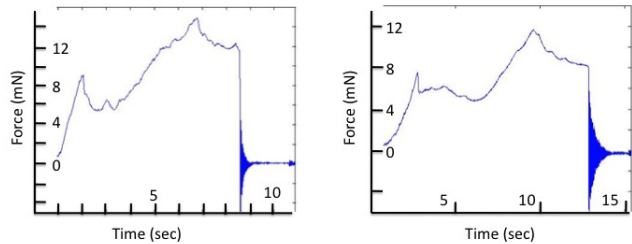


Fig. 11. Membrane peeling using free hand (left) and the Eye Robot (Right); Force vs Time

Measured forces from 8 trials for each method in two events are shown in Fig. 12. We can see that force in robot-assisted manipulation is slightly smaller than that by free hand. But the deviation from the robot-assisted manipulation forces is relatively larger than the free hand one; this may be due to the learning curve of using the robot. This will be the subject of future study. The main point in the current initial pilot study was to verify that we could obtain useful data with our sensor technology.

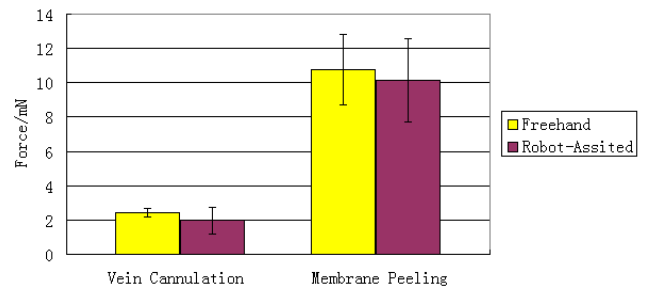


Fig. 12. Peak force measurements in Vein Cannulation and Membrane peeling.

During the wavelength-to-force conversion, data collected in the first second were averaged to be the reference value. It is notable that for free hand and robot-assisted data, the base wavelengths of the FBG are slightly different. This is because, the data for free hand and robot-assisted were collected in separate days. This shift in wavelength may be due to the temperature differences. Overall, the sensor gave consistent readings for the load-free condition in each single trial.

This paper has reported the initial development and preliminary evaluation data for a new family of force-sensing microsurgical instruments. These experiments have shown that placing FBG fiber optic force sensors along the shaft of millimeter-diameter retinal instruments can produce sufficient force sensitivity to measure the extremely delicate forces associated with retinal surgery while also avoiding the confounding factor of tool-to-sclera interaction forces. Other advantages associated with our approach include robustness, versatility, immunity to electrical noise, and relatively easy interfacing and sterilization.

Our immediate goals for the future include design of a family of 2 DOF sensing tools with a variety of end-effectors, including the simple pick and tweezers illustrated in Fig. 1, above. As this is written in September 2008, design studies for these tools are underway, and fabrication is expected in the next couple months.

Although the simplest design approach places 2 FBG sensors at 90° separation along the tool shaft, we are also considering redundant configurations with 3 or 4 sensors distributed evenly around the shaft. Such configurations will balance out the effects of the FBG sensors on the mechanical properties of the titanium tool shafts and will also provide means for compensating for temperature effects.

The dynamic response is one area that will be investigated to increase the overall sensor sampling rate to at least twice that of the human hand tremor frequency. For robotic applications, faster (e.g., 50 Hz) measurement rates are desirable.

The axial force measurement is still desirable for a complete a 3-DOF force sensing tool, though the sensitivity in measuring the strain in axial direction is much smaller compared to those along the transverse plane. Further investigation of the necessity of the extra DOF and possible solutions is currently in progress.

As soon as these tools are available, we plan to begin a much more extensive series of studies to measure baseline tool-to-tissue forces during retinal procedures, as well as to develop sensory substitution and force-based virtual fixtures for assisting the surgeon in carrying out these procedures.

Examples of the former would include auditory or visual force cues (e.g., on a surgical microscope display). Examples of the latter include force servoing and force limiting behaviors to improve safety.

ACKNOWLEDGMENT

The authors would like to thank Brian Hu for his assistance in software sensor development and data collection.

The author Zhenglong Sun would like to thank Prof Louis Phee from School of Mechanical and Aerospace Engineering, Nanyang Technological University, Singapore, for his financial sponsorship during this project.

- [1] M. Patkin, "Ergonomics applied to the practice of microsurgery," *Aust NZ J Surg*, Vol. 47, pp. 320-329, 1977.
- [2] P.K. Gupta, P.S. Jensen, and E. de Juan, Jr., "Surgical forces and tactile perception during retinal microsurgery," *MICCAI '99, LNCS 1679*, pp. 1218-1225, 1999.
- [3] I. Iordachita et al, "Steady-Hand manipulator for retinal surgery," In proceedings, *MICCAI Medical Robotics Workshop, 2006*
- [4] B. Mitchell et al, "Development and Application of a New Steady-Hand Manipulator for Retinal Surgery," *IEEE Int Conf on Robotics and Automation, 2007*. pp. 623-629.
- [5] Y. Zhou, B.J. Nelson, and B. Vikramaditya, "Fusing force and vision feedback for micromanipulation," *Proc. IEEE Int. Conf. Robotics & Automation*, Leuven, Belgium, pp. 1220-1225, May 1998.
- [6] K. Kim, Y. Sun, R. Voyles, B. Nelson, "Calibration of Multi-Axis MEMS force Sensors Using the Shape-From-Motion Method", *IEEE Sensors Journal*, Vol 7, No. 3, March 2007.
- [7] A. Menciassi, A. Eisenberg, G. Scalari, C. Anticoli, M.C. Carrozza, and P. Dario, "Force feedback-based microinstrument for measuring tissue properties and pulse in microsurgery," *Proc. IEEE Int. Conf. Robotics & Automation*, Seoul, Korea, pp. 626-631, May 2001.
- [8] P.J. Berkelman, L.L. Whitcomb, R.H. Taylor, and P. Jensen, "A miniature microsurgical instrument tip force sensor for enhanced force feedback during robot-assisted manipulation," *IEEE Trans. Rob. Autom.*, Vol. 19, No. 5, pp. 917-921, 2003.
- [9] P. J. Berkelman, L. L. Whitcomb, R. H. Taylor, and P. Jensen, "A miniature Instrument Tip Force Sensor for ro-bot/Human Cooperative Microsurgical Manipulation with Enhanced Force Feedback," in *Medical Image Computing and Computer-Assisted Interventions*, Pittsburgh, 2000, pp. 897-906.
- [10] A. D. Jagtap and C. N. Riviere, "Applied Force during Vitreoretinal Microsurgery with Handheld Instruments," in *Proc. 26th IEEE Engineering in Medicine and Biology Conference (EMBS)*, San Francisco, 2004, pp. 2771-2773.
- [11] K.O. Hill and G. Meltz, "Fiber Bragg grating technology fundamentals and overview," *Journal of Lightwave Technology*, Vol. 15, No. 8, pp. 1263-1276, 1997.
- [12] T. Leng, J.M. Miller, K.V. Bilbao, D.V. Palanker, P. Huie, and M.S. Blumenkranz, "The chick chorioallantoic membrane as a model tissue for surgical retinal research and simulation," *Retina*, Vol. 24, No. 3, pp. 427-434, June 2004.